



## RESEARCH ARTICLE

**Pb (II) Recovery by Trout Bones: Adsorption, Desorption and Kinetic Study**

Beyhan Kocadagistan\*

Atatürk University, Faculty of Engineering, Department of Environmental Engineering, Erzurum/Türkiye

## ARTICLE INFO

**Article History**

Received: 24.10.2022

Accepted: 21.11.2022

First Published: 22.12.2022

**Keywords**

Adsorption kinetics

Desorption

Lead removal

Rainbow trout



## ABSTRACT

Heavy metal removal from the water was studied by using fish bones produced in the trout farm of Atatürk University Faculty of Fisheries. Fish bones used as adsorbent were obtained from rainbow trout (*Oncorhynchus mykiss*). Trout bone was used in its natural form. According to the experimental results that maximum Pb (II) adsorption capacity of rainbow trout bones was 188.16 mg/g. The Langmuir, Freundlich, and Temkin isotherm models were applied to describe the adsorption of Pb (II) on trout bones. Langmuir and Freundlich isotherm models were found more favourable than Temkin with the correlation coefficients of 0.999, 0.999, and 0.857, respectively. Controllable factors used in this study were solution pH, temperature, adsorbent dosage, mixing speed, and initial Pb (II) concentration. The optimum working parameter values for Pb (II) adsorption using trout bones were found to be 5.5, 30 °C, 3 g/L, 200 rpm, and 10 mg/L for pH, temperature, adsorbent concentration, stirring speed, and initial Pb (II) concentration, respectively. The adsorption kinetics of Pb adsorption by trout bones was modelled using the pseudo-first order and the pseudo-second order kinetics equations. The results indicate that, pseudo-second-order kinetic model gives more favourable results ( $R^2_{\text{mean}} = 0.997$ ) than pseudo-first-order ( $R^2_{\text{mean}} = 0.971$ ). Fish bones were characterized by some instrumental analyses such as SEM, EDS, FTIR, and zeta potential measurements. In the regeneration phase of the study, maximum desorption efficiency was 95.86% at pH 1.5.

**Please cite this paper as follows:**

Kocadagistan, B. (2022). Pb (II) recovery by trout bones: Adsorption, desorption and kinetic study. *Journal of Agricultural Production*, 3(2), 88-99. <https://doi.org/10.56430/japro.1193955>

**Introduction**

Heavy metals are more commonly known as metals and their compounds having an atomic density greater than  $4\pm 1$  g/cm<sup>3</sup>. Cu, Zn, Hg, Cd, Pb, Sn, Mn, As, Cr, Co, Ni, and Ag can be counted as heavy metals, which are considered the most common toxic mineral pollutants in water and soil systems (Nadeem et al., 2006). Many of these substances have been blacklisted by various international organizations as they cause soil and water pollution (Edelstein & Ben-Hur, 2018; L. Liu et al., 2018; Chen et al., 2021). Heavy metals cause significant damage to human health because of their accumulation properties and difficult decomposition. Methods such as chemical precipitation, electrochemical and redox removal, ion exchange, adsorption and membrane separation are frequently used to remove heavy metals from wastewater (Demirbas,

2008). Lead is one of the most detected pollutants in aqueous environments and soils. It is used as a raw material for a wide variety of industries, especially battery manufacturing (Abdelhafez & Li, 2016; L. Liu et al., 2018; Chen et al., 2021). Lead concentrations in most bodies of water on the planet are above the EPA's action level of 15 ppb. Removal of this toxic metal from aquatic environments such as drinking water, stream water, groundwater, and wastewater is very important for human life (Abdelhafez & Li, 2016). The type, form, and concentration of lead or any other heavy metal in water and wastewater play a decisive role in the selection of treatment processes to be designed to remove them.

In the literature, there are many traditional and new wastewater treatment methods such as chemical precipitation (Kumar et al., 2021), micro, ultra, and nanofiltration (Abdullah

\* Corresponding author  
E-mail address: beyhank@atauni.edu.tr

et al., 2019), electrochemical oxidation (Martínez-Huitle & Panizza, 2018), ion exchange (Dąbrowski et al., 2004), and adsorption (Senthil Kumar & Gayathri, 2009; Basu et al., 2017; R. Liu et al., 2018; Lu et al., 2019; Zhu et al., 2019) for lead removal from water and wastewater. Among these methods, adsorption is one of the most used techniques in heavy metal removal due to its high efficiency and low cost (Hayati et al., 2017).

One of the factors limiting the widespread use in adsorption processes is the determination of adsorbent with high adsorption capacity but low cost. Therefore, adsorbents obtained from natural sources have attracted great interest (Silva-Yumi et al., 2018). There are many heavy metal adsorption studies in the literature, especially with adsorbents obtained from natural sources such as agricultural wastes and their modified forms (Dubey & Gopal, 2007; Bansal et al., 2009; Qiao et al., 2019; Yu et al., 2022), wheat straw (Khan et al., 2021), biochar (Q. Wang et al., 2018; Guan et al., 2022), clay (Xie et al., 2018), tea plant waste (Ibrehem, 2019).

In heavy metal removal processes by adsorption, another important point is that heavy metal ions retained by adsorption are not released back into the nature after the process. Because the metal binding mechanism is mostly by chemical adsorption, the adsorbed metal can be desorbed under suitable conditions (Tongtavee et al., 2021). Performing desorption in a controlled manner can turn this situation into an advantage and the materials left behind after adsorption can be recovered in an efficient, economical, and environmentally friendly way. Also, desorption is an environmentally friendly technique with low energy consumption and due to the reversible nature of most adsorption processes, adsorbents can be used repeatedly with simple desorption methods (Charoenchai & Tangbunsuk, 2022).

Aquaculture is an alternative food that meets the protein needs of the increasing world population. Fish bones are an important part of the wastes generated in fish production facilities, which are becoming increasingly widespread throughout the world. Global production of aquatic animals was around 178 million tons in 2020. About 51% (90 million tons) of this amount was fisheries. In addition, 63 percent (70 percent from caught fishing and 30 percent from aquaculture) of the total production was harvested in marine waters and 37 percent (83 percent from aquaculture and 17 percent from hunting) from inland waters (FAO, 2022). In 2021, 335,644 tons of aquaculture production in Türkiye took place in the seas and 136,042 tons in inland waters. The most important fish species grown were trout with 135,732 tons in inland waters, sea bass with 155,151 tons and sea bream with 133,476 tons in seas (TÜİK, 2022). In addition, aquaculture contributes more than 53 percent to world aquaculture production, which is worth 232 billion USD (FAO, 2022).

In this study, rainbow trout bones (RTB) was selected and tested as an adsorbent for waste recycling. It is thought that it is very interesting to use the bones of rainbow trout, which is a fish species that can live in clean waters, to clean the water.

The aim of this study is to investigate the usability of RTB for Pb (II) removal via adsorption. In this way, it is thought that an effective and reusable natural novel metal ion adsorbent will be presented to the field of application. Regeneration processes have not been studied much in order to reuse the adsorbents used in adsorption studies, which are frequently encountered in the literature. It is thought that the study will contribute to the literature in terms of waste minimization and evaluation. In order to achieve this aim, the effects of operating parameters such as pH, temperature, stirring speed, time, adsorbate, and adsorbent concentrations on adsorption were investigated in detail. In addition, Scanning Electron Microscopy (SEM), Fourier Transform Infrared Spectroscopy (FTIR) and Brunauer-Emmett-Teller (BET) analyses for rainbow trout bones were made and presented to the literature. With the help of kinetic models, the adsorption behaviour of these bones was also tried to be revealed.

## Materials and Methods

### Chemicals

In experimental studies, aqueous  $\text{Pb}(\text{NO}_3)_2$  was used as a stock solution at a concentration of 1000 mg/L Pb (II). HCl and NaOH solutions were used for pH adjustment and  $\text{HNO}_3$  solutions were used for regeneration experiments. All chemicals were analytical reagent grade from E. Merck, Darmstadt, Germany.

### Adsorbent

In the study, artificial pond rainbow trout bones and vertebrae were used as adsorbent and this material was obtained from Atatürk University Fisheries Faculty Inland Water Fish Application and Research Centre.

RTB were first separated from their meat as much as possible, washed with hot water many times to remove their fat, and then dried in an oven at 105 °C by washing with distilled water. Then, to remove organic residues (oil and fatty acids), ethanol was added and mixed in a shaker for two hours at room temperature. This process was repeated three times and the bones were washed with distilled water and dried. After this process, all RTB that became brittle were powdered and kept in a desiccator from a humid environment until the experiments were carried out. Mineral and chemical composition of RTB were given in Table 1.

**Table 1.** Mineral composition of RTB lipid free dry matter (Toppe et al., 2007).

Mineral		Quantity
Calcium	g/kg	147
Phosphorus	g/kg	87
Magnesium	g/kg	2.4
Iron	mg/kg	32
Zinc	mg/kg	126
Copper	mg/kg	0.9
Chromium	mg/kg	6.7
Sodium	g/kg	5.8
Potassium	mg/kg	7.7
Selenium	mg/kg	-
Iodine	mg/kg	2.5
Chlorine	g/kg	4.2
Fluorine	g/kg	0.09
Arsenic	mg/kg	1.2
Cadmium	mg/kg	0.02
Mercury	mg/kg	0.01
Lead	mg/kg	-

### Analyses

CrisonpH25<sup>+</sup> brand pH meter device was used. Samples were centrifuged before analyses with Nüve NF 1200R centrifuge device. Pb (II) concentrations were measured at 283.3 nm wavelength, 10 mA current and 0.5 nm slit width by using a Shimadzu AA6800 atomic adsorption spectrophotometer. Scanning Electron Microscopy (ZEISS SIGMA 300), Fourier-Transform Infrared Spectroscopy (Bruker VERTEX 70v), Brunauer-Emmett-Teller (Micromeritics 3 Flex), and Zeta potential (Malvern Zetasizer Nano ZSP) analyses were performed to reveal adsorbent characterization. These analyses were carried out in the laboratories of Atatürk University Eastern Anatolia High Technology Application and Research Centre (DAYTAM).

Analyses throughout the study were carried out in triplicate and carried out according to the standard methods (Rice et al., 2012). The results presented in the article are the average of repetitions. In addition, error function analyses were used in isotherm and kinetic model calculations for the reliability of the results.

### Adsorption Experiments

Adsorption experiments were carried out with 100 mL Erlenmeyer flasks. During the experiments, initial Pb (II) concentrations were between 10 and 200 mg/L. The pH values were used between 2 and 12 and the adsorbent concentrations were between 0.25 and 3 g/L. Solution temperatures were maintained between 20 °C and 40 °C in a thermoregulated shaker (Edmund Bühler Incubator HoodTH15) and mixing

speeds and times were applied in the range of 100 to 300 rpm and 1 to 300 minutes, respectively.

Adsorbed Pb (II) amount onto per unit weight of adsorbent (mg/g) is calculated with the following equation (Bardestani et al., 2019):

$$q_e = \frac{(C_o - C_t) \cdot V}{m} \quad (1)$$

where,  $C_o$  and  $C_t$  are the Pb (II) concentrations (mg/L) at time 0 and  $t$ , respectively;  $V$  is the volume of the Pb (II) solution (L); and  $m$  is the weight of material (g).

### Desorption Experiments

The suitability of an adsorbent for regeneration is an important factor in addition to its properties such as adsorption capacity or cost. For this reason, the RTB used in this study were subjected to desorption experiments to measure whether they could be reused or not, in addition to examining their adsorption capacity.

Desorption experiments continued with the process of taking the adsorbent into a 0.1 M HNO<sub>3</sub> solution/distilled water mixture after the adsorption process reached equilibrium and regenerating it under mechanical stirring at 200 rpm for 8 hours at room temperature. The amount of lead transferred to the solutions in this way was measured at different time intervals.

In order to reveal the pH effect, the pH range of the regeneration solution was changed as in the adsorption process. In the study, adsorption and desorption processes were considered as a whole and this procedure was carried out for all samples immediately after the completion of the adsorption process.

## Results and Discussion

### The Effect of Operational Parameters

pH affects the electronic equilibrium on non-covalent bonds and destabilizes the electronic configuration in the medium. Therefore, it is one of the most important physicochemical parameters in adsorption processes. Low pH solutions contain high concentrations of hydronium cations and compete for a significant number of functional groups interacting with light metals or other metal cations (Cid et al., 2020). As the pH increases, the more negatively charged ligands are depleted and then metallic cations are attracted to the cell surface, resulting in binding (Yun et al., 2001). Finding the optimum adsorption pH is very important as pH affects the removal of metal ions from aqueous solutions by influencing the chemistry of metals and changing the surface charge of particles (Asadi et al., 2020). At the same time, pH is an important parameter in desorption, although not as much as in adsorption, since the amount of heavy metal recovered as a result of the desorption process also depends on the amount of heavy metal retained by

the adsorption process. General desorption is controlled by both metal desorption and re-adsorption reactions.

In metal ion adsorption processes, as the pH rises to the neutral zone and above, metal compounds begin to precipitate in the solution; on the contrary, the adsorbent surface is positively charged and does not attract metal ions. In both cases, the adsorption efficiency falls outside the optimum value. Therefore, Zeta Potential values of adsorbent against pH are

very helpful to find the optimum pH value. In a solution containing Pb (II) ions, below pH 3.30, the dominant type is Pb (II) ions in the solution, while lead will begin to precipitate as Pb(OH)<sub>2</sub>, as the pH starts to rise (Awual & Hasan, 2019).

Zeta Potential values of RTB for different pH values are given in Figure 1. As seen in the figure, positive and negative peak values were measured as +18 mV and -236 mV at pH 2 and 14, respectively.

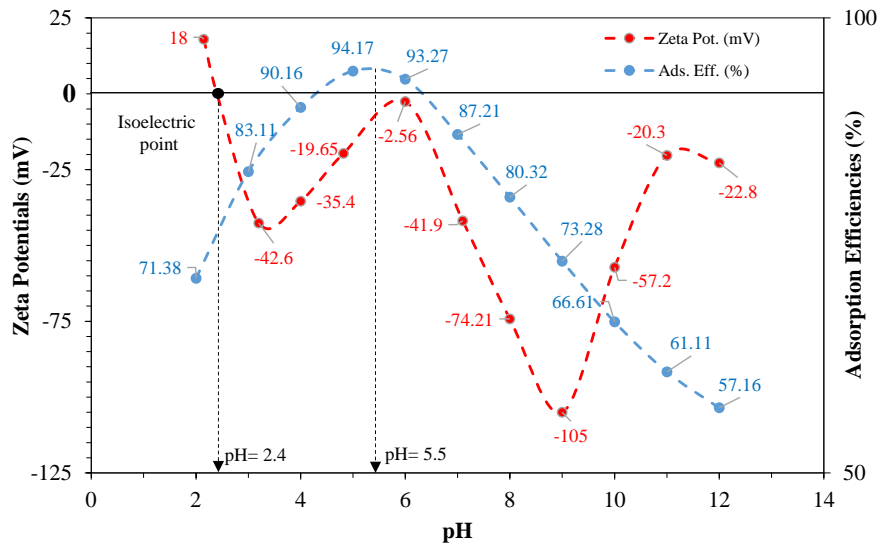


**Figure 1.** pH versus zeta potential and adsorption efficiencies graph of RTB.

As can be seen from the graph, the zeta potential values of RTB at different pH values have a wide range from +18 mV to -105 mV. However, when evaluated together with the adsorption efficiencies [for 3 g/L adsorbent, 10 mg/L initial Pb (II) concentration, and 30 °C conditions] obtained at these pH values, it is seen that the highest efficiency is obtained at pH 5.5. The zeta potential value was measured as -7 mV at the pH value where this yield was obtained. Theoretically, at higher negative potential values, positively charged lead ions should bind more to the adsorbent. However, as mentioned above, this is not always the case in metal chemistry. Because at high pH values (pH 5 and above) where higher potential values are obtained, precipitation occurs in the solution and the adsorption efficiency decreases (Y. Wang et al., 2013). Therefore, pH 5.5 was chosen as the optimum value in the study.

Lead concentrations of 10, 25, 50, 100, and 200 mg/L were applied to evaluate the effect of the initial Pb (II) concentration on adsorption. Adsorption efficiencies versus time at different initial Pb (II) concentrations are given in Figure 2.

As seen in Figure 2, the amount of Pb (II) remaining in the solution increased with increasing initial concentration, and the adsorption efficiency decreased at the same rate. Maximum adsorption efficiencies were found as 87.4, 84.56, 85.21, 80.79, and 70.5% for 10, 25, 50, 100, and 200 mg/L initial Pb (II) concentrations, respectively. According to these results, the

optimum initial Pb (II) concentration was determined as 10 mg/L. The case of higher adsorption efficiency at low initial concentrations can be explained by the fact that when the initial concentration of metal ions is low, there are many adsorption sites on the adsorbent surface and metal ions can fully react with the adsorption sites. Therefore, the removal rate is higher (Chen et al., 2021).

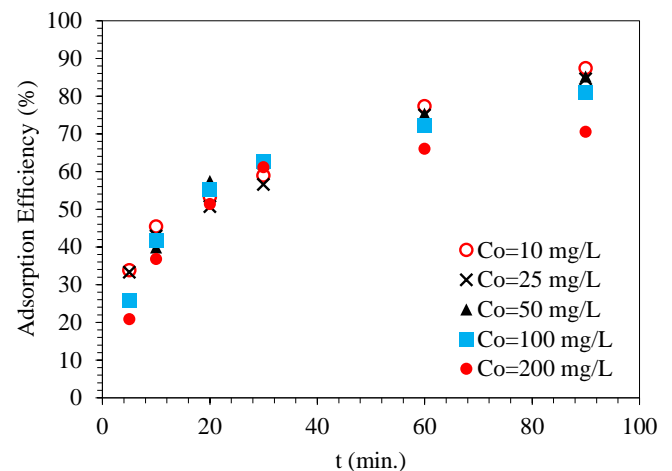


**Figure 2.** Pb (II) removal efficiencies versus time for different initial Pb (II) concentration (m = 3 g/L, pH = 5.5, T = 30 °C, agitation speed = 200 rpm).

Figure 3 shows the change in the Pb (II) removal rates when the adsorbent dosage is changed from 1 mg/L to 3 mg/L. As can be seen in Figure 3, the concentration of Pb (II) remaining in the solution decreases (removal rates increases) as the adsorbent dosage increases from 1 to 3 g/L due to the presence of more adsorbent surface area in the solution. With the increasing adsorbent concentration, there was not a big difference in the removal efficiencies at equilibrium, but the highest yield was obtained with 3 g/L RTB concentration. As it can be seen when Figure 3 is examined, while the removal efficiency is about 78% at 0.25 g/L adsorbent concentration, this value reached a maximum of 87.4% at 3 g/L.

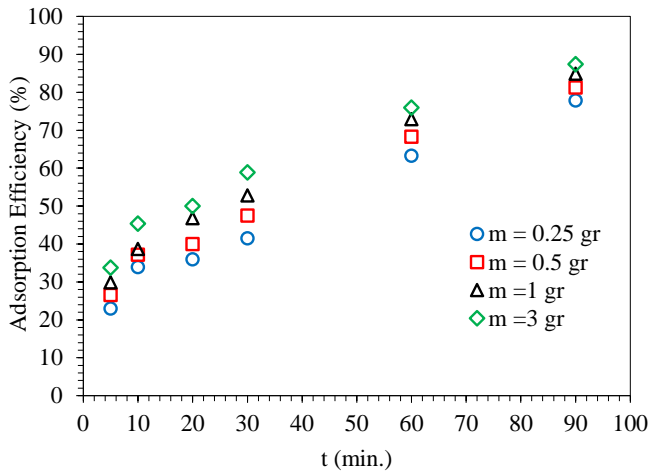


**Figure 3.** Pb (II) removal efficiencies versus time for different adsorbent concentration ( $C_o = 10$  mg/L, pH = 5.5, T = 30 °C, agitation speed = 200 rpm).

Shaker speeds were varied between 100 rpm and 300 rpm to reveal how the mixing speed affected the adsorption. As can be seen from Figure 4, the amounts of Pb (II) concentrations remaining in the solution are lower at 100 and 200 rpm than at 250 and 300 rpm. The highest removal efficiency was obtained at 200 rpm and decreased with increasing speed, since high mixing speeds caused the boundary layer to decrease and the bed resistance to decrease, resulting in a decrease in the amount of adsorbed material (Taha et al., 2016).

Temperature has a significant effect on the adsorption efficiency. In the study, the experiments were carried out at three different temperatures ranging from 20 to 40 °C. As can be seen in Figure 5, the temperature increases from 20 °C to 30 °C positively affected the adsorption efficiency. However, the efficiency decreases as the temperature rises from 30 °C to 40 °C. This is due to the exothermic nature of the process or the reduced effect of physical forces at high temperature (Kennedy et al., 2007).

As a result of the data obtained in studies examining the effects of operational parameters on adsorption, the most suitable operating parameter values for Pb (II) adsorption using RTB, temperature, adsorbent concentration, mixing speed, and

initial Pb (II) concentration were 30 °C, 3 g/L, 200 rpm, and 10 mg/L, respectively.

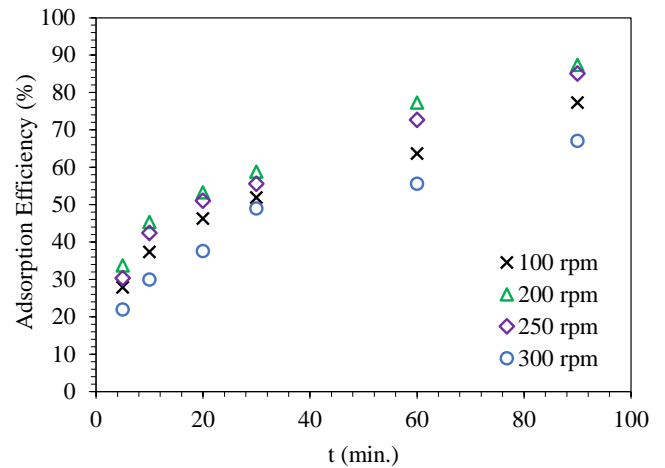


**Figure 4.** Pb (II) removal efficiencies versus time for different agitation speed ( $C_o = 10$  mg/L, m = 3 g/L, pH = 5.5, T = 30 °C).

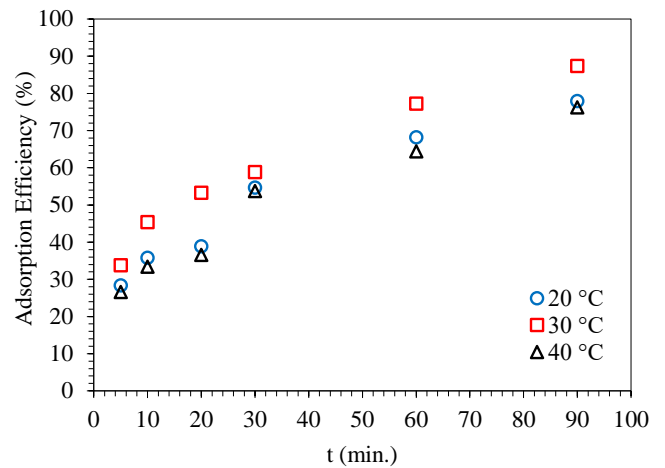


**Figure 5.** Pb (II) removal efficiencies versus time for different temperature ( $C_o = 10$  mg/L, m = 3 g/L, pH = 5.5, agitation speed = 200 rpm).

**Adsorbent Characterization**

Scanning Electron Microscopy (SEM), Fourier-Transform Infrared Spectroscopy (FTIR), and Brunauer-Emmett-Teller (BET) analyses were performed to examine the characteristic structure of RTB. BET and Langmuir surface area of RTB are 1.86 and 2.08 m<sup>2</sup>/g, respectively. The other values obtained by BET analyse are given in Table 2.

**Table 2.** BET analyse values of RTB.

Parameter	Size
BET surface area (m <sup>2</sup> /g)	1.8660±1.4511
Langmuir surface area (m <sup>2</sup> /g)	2.0847
g-Plot micropore area (m <sup>2</sup> /g)	0.9102
g-Plot out surface area (m <sup>2</sup> /g)	0.9558
Mean particle size (ηm)	3.215, 3.546
Mean particle diameter (ηm)	1.4410
Maximum pore volume (cm <sup>3</sup> /g)	0.176931750



It was observed that the values of the peaks, which were 3250, 2982, 1155, 1500, 1020.552 before Pb (II) adsorption, shifted to 3300, 2980, 1587, 1510, 1025.555 cm<sup>-1</sup> values after adsorption corresponded to the O-H and C-H groups. These groups can generally be alcohol, phenol, carboxyl acids. It has been observed that C-H and C-C groups may be present in the band range of 500-1000 cm<sup>-1</sup> at 552-1020 cm<sup>-1</sup> peaks before adsorption and at 552-1025 cm<sup>-1</sup> peaks after adsorption. C=O and C=N functional groups were observed at 1510 and 1587 cm<sup>-1</sup> values.

**Adsorption Isotherms**

Adsorption isotherms represent the amount of substance adsorbed per unit of adsorbent as a function of equilibrium concentration in solution at constant temperature. In this study, three isotherm equations; namely Langmuir, Freundlich, and Temkin were tested. The equations for these isotherms (Senthil Kumar & Gayathri, 2009) are given below.

Langmuir model equation:

$$q_e = \frac{q_m K_L C_e}{1 + K_L C_e} \tag{2}$$

where,  $q_m$  is the maximum adsorbate uptake capacity (mg/g) and  $K_L$  is the Langmuir constant related to the energy of adsorption (L/mg).

Freundlich model equation:

$$q_e = K_F C_e^{\frac{1}{n}} \tag{3}$$

where,  $K_F$  is Freundlich constant related to biosorption capacity (L/g) and  $1/n$  is the heterogeneity factor.

Temkin model equation:

$$q_e = B \ln AC_e \tag{4}$$

where,  $B = RT/b$ ,  $b$  is the Temkin constant related to heat of sorption (J/mol),  $A$  is the Temkin isotherm constant (L/g),  $R$  is the gas constant (8.314 J/mol.K), and  $T$  is the absolute temperature (K) of solution.

Besides, the essential property of the Langmuir isotherm can be expressed in terms of the dimensionless constant separation factor  $R_L$  and values between  $0 < R_L < 1$  represent a favourable adsorption (Al-Ghamdi et al., 2019).

$$R_L = \frac{1}{1 + K_L C_o} \tag{5}$$

In the batch equilibrium experiments, the temperature was 20 to 40 °C, the adsorbent dosage was 0.25 to 3 g/L, and the initial Pb (II) concentration was 10 to 200 mg/L. Figure 8 shows the linear model plots of the isotherms for 30 °C, pH 5.5, and 200 rpm operating conditions. Isotherm model parameters are given in Table 3.

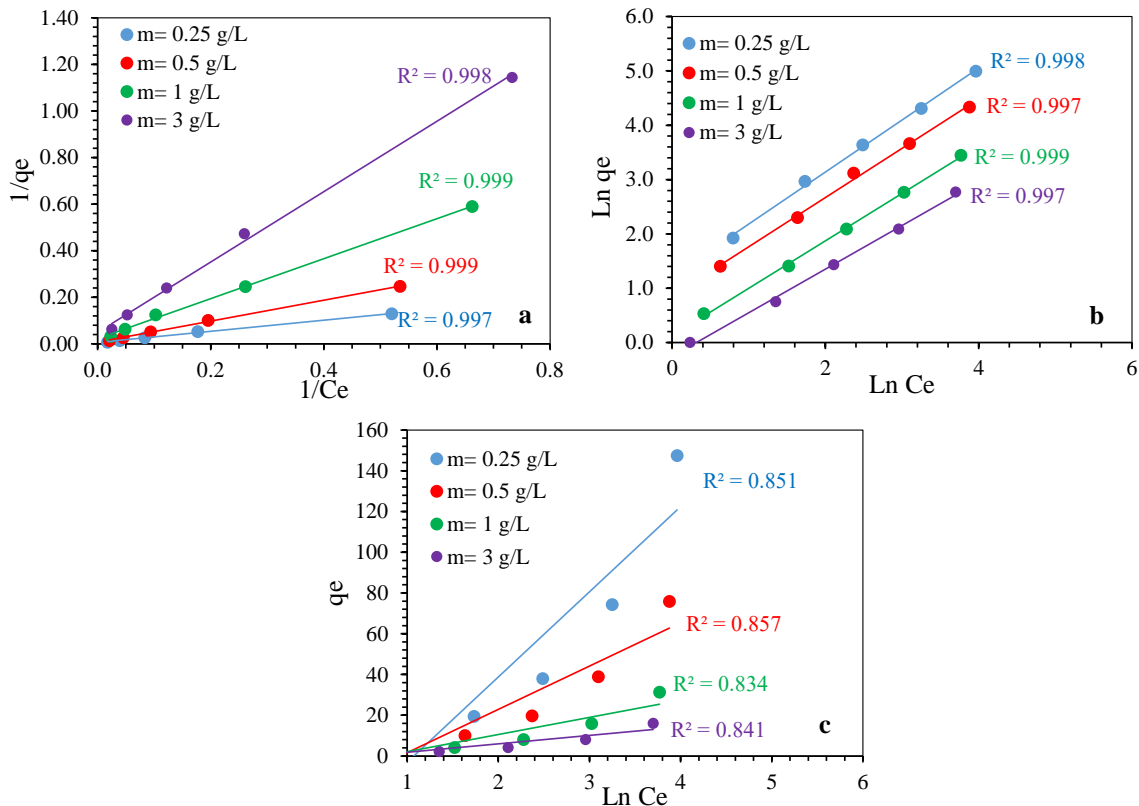


**Figure 8.** Langmuir (a), Freundlich (b), and Temkin (c) isotherm model plots 30 °C, pH 5.5, and 200 rpm agitation speed operating conditions.

**Table 3.** Isotherm model parameters of Pb (II) adsorption on RTB for various adsorbent dosages at 30 °C.

Parameters	Values			
	0.25	0.5	1.0	3.0
Langmuir				
$q_m$ (mg/g)	188.16	140.19	44.94	20.38
$K_L$ (L/mg)	0.022	0.016	0.026	0.033
$R^2$	0.997	0.999	0.999	0.998
ARE	6.213	5.675	8.147	5.121
SSE	0.027	0.016	0.031	0.024
$\chi^2$	0.321	0.267	0.334	0.286
Freundlich				
$K_F$ (L/g)	3.411	2.355	1.136	0.778
$1/n$	0.956	0.907	0.872	0.802
$R^2$	0.998	0.997	0.999	0.997
ARE	7.150	6.666	7.175	6.045
SSE	0.033	0.027	0.029	0.031
$\chi^2$	0.463	0.341	0.339	0.317
Temkin				
$A$ (L/g)	0.342	0.397	0.476	0.575
$b$ (J/mol)	62.28	122.35	310.36	631.66
$R^2$	0.851	0.857	0.834	0.841
ARE	8.662	6.791	9.124	7.821
SSE	0.161	0.078	0.082	0.101
$\chi^2$	0.527	0.395	0.429	0.463

It can be seen from Table 3 that the  $R^2$  correlation coefficients of the Langmuir and Freundlich are higher than the Temkin. On the other hand,  $R^2$  values obtained for Langmuir model (0.998 on average) were slightly higher than Freundlich (0.997 on average) for the trials performed under the same conditions. As can be seen from Table 3, the correlation coefficients of the Temkin isotherm model have the smallest values obtained in the study and it stands out as the least suitable model for the adsorption of lead on RTB among other

models examined in this study (between 0.834 and 0.857). Therefore, it can be said that Langmuir and Freundlich models are suitable for the adsorption of Pb (II) on RTB. On the other hand, it can be said that the Pb (II) adsorption on RTB is favourable since  $K_L$  values of Langmuir and  $1/n$  values of Freundlich were smaller than 1 for all operating conditions (Zhang et al., 2019). For all conditions in this study, the calculated dimensionless constant  $R_L$  was between 0 and 1. This reveals that adsorption is favourable. Error analyses also confirm this situation due to smaller error values and shown in Table 3.

### Adsorption Kinetics

Pseudo-first-order and pseudo-second-order kinetic models were used to reveal the reaction rate. And to make the results more useful, these models were analysed in both linear and nonlinear forms. Equations of these models are given in Eq. (6) and (7), respectively (Senthil Kumar & Gayathri, 2009).

$$q_t = q_e [1 - \exp(-k_1 t)] \quad (6)$$

$$q_t = \frac{q_e^2 k_2 t}{1 + (k_2 q_e t)} \quad (7)$$

where,  $k_1$  (1/min) and  $k_2$  (g/mg.min) are the adsorption rate constants of first-order and second-order kinetic models, respectively;  $q_e$  is the equilibrium adsorption uptake (mg/g); and  $q_t$  is the adsorption uptake (mg/g) at time  $t$  (min). Results of the kinetic study are given in Table 4 for 30 °C. Figure 9 shows the linearised pseudo-first-order (a) and pseudo-second-order (b) model plots at 30 °C, pH 5.5, and 200 rpm agitation speed operating conditions. Error analyses results for kinetic adsorption are given in Table 5.

**Table 4.** Kinetic model parameters for 30 °C.

M (g)	$C_o$ (mg/L)	$q_{e,exp}$ (mg/g)	Pseudo-First-Order		Pseudo-Second-Order			
			$k_1$	$R^2$	$q_{e,cal}$	$k_2$	$R^2$	$q_{e,cal}$
0.25	10	31.160	0.0228	0.960	24.554	0.0019	0.997	34.756
	25	77.360	0.0245	0.951	61.944	0.0008	0.996	83.084
	50	151.960	0.0314	0.952	120.344	0.0003	0.996	184.097
	100	297.000	0.0387	0.973	233.426	0.0002	0.999	349.598
	200	589.800	0.0461	0.997	532.839	0.0001	0.998	716.875
0.5	10	16.260	0.0252	0.972	12.554	0.0039	0.997	18.458
	25	39.760	0.0272	0.969	30.985	0.0015	0.991	44.983
	50	78.640	0.0292	0.924	57.713	0.0006	0.994	92.504
	100	155.680	0.0346	0.969	115.227	0.0004	0.999	180.359
	200	303.460	0.0406	0.989	254.319	0.0002	0.999	363.920
1	10	8.490	0.0271	0.985	6.438	0.0062	0.992	9.734
	25	20.430	0.0293	0.986	15.370	0.0031	0.993	22.973
	50	40.270	0.0353	0.970	30.102	0.0014	0.999	46.590
	100	79.430	0.0325	0.960	55.483	0.0008	0.998	90.323
	200	156.710	0.0346	0.974	120.760	0.0003	0.999	184.523
3	10	2.913	0.0293	0.987	2.041	0.0322	0.993	3.154
	25	7.047	0.0297	0.986	5.024	0.0116	0.996	7.743
	50	13.927	0.0346	0.975	10.006	0.0045	0.999	15.882
	100	26.930	0.0324	0.967	18.237	0.0026	0.998	30.255
	200	53.210	0.0345	0.977	40.709	0.0010	0.999	62.388

According to the pseudo-first-order kinetic model, the adsorption rate is controlled by the liquid membrane diffusion. On the other hand, the pseudo-second-order kinetic model assumes that the rate is controlled by chemical adsorption. From Table 4, it is seen that the pseudo-second-order kinetic model correlation coefficients are higher than the pseudo-first-order correlation coefficients. Therefore, it can be said that the pseudo-second order kinetic model is more suitable for the adsorption of Pb (II) on RTB. The calculated  $q_e$  values of model ( $q_{e,cal}$ ) were closer to the experimental measured  $q_e$  values ( $q_{e,exp}$ ) in pseudo-second-order model, which indicates that the adsorption is controlled by chemical adsorption. Moreover, the smaller the adsorption rate constants ( $k$ ), the stronger the affinity of the adsorbent region, so the adsorption process is faster and more convenient (Chu et al., 2019). The pseudo-

second-order kinetic model rate constants obtained in this study were the smallest, which is further proof that this kinetic model is more suitable.

**Table 5.** Error analysis results of kinetic adsorption for 30 °C.

$C_o$ (mg/L)	10	25	50	200
Pseudo-First-Order				
ARE	26.6	33.1	36.8	41.9
SSE	0.531	0.618	0.771	0.734
$\chi^2$	3.27	3.21	2.98	2.69
Pseudo-Second-Order				
ARE	8.21	7.75	6.32	8.13
SSE	0.223	0.193	0.136	0.097
$\chi^2$	0.421	0.367	0.441	0.384

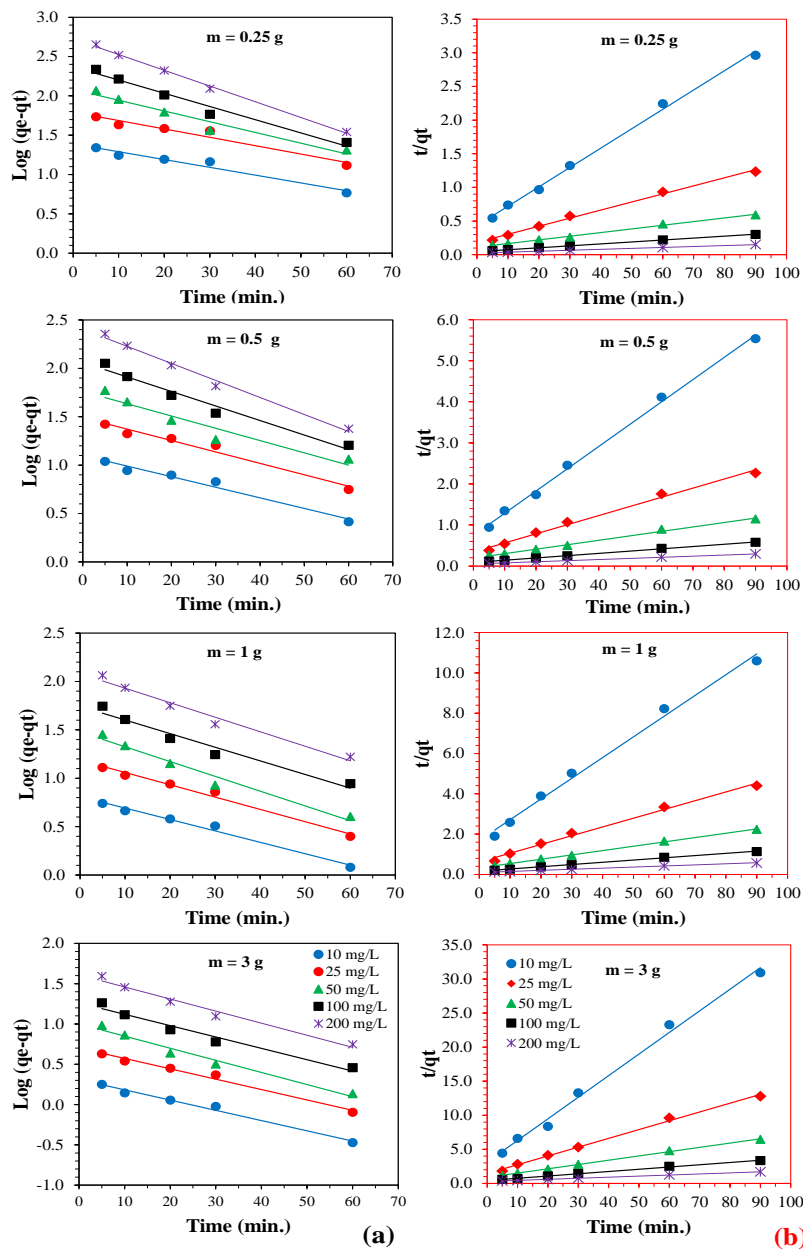


**Figure 9.** Pseudo-first-order (a) and pseudo-second-order (b) kinetic model plots at 30 °C, pH 5.5, and 200 rpm agitation speed operating conditions.

## Regeneration

For the measurement of desorption capacity of RTB samples used in adsorption, samples obtained from batch adsorption experiments were filtered through filter paper and rinsed with distilled water 3 times to remove free Pb (II) and placed in solutions brought to different acidic pH values using 0.1 M HNO<sub>3</sub>. Samples were taken from the solutions and Pb (II) analyses were performed. As a result of the analysis, the desorption ratio RTB was calculated with the following equation (Eq. 8):

$$\text{Des. ratio} = \frac{VC}{mq_e} \times 100\% \quad (8)$$

where,  $V$  is the volume of the desorption solution (L);  $C$  is the Pb (II) concentration in the desorption solution (mg/L);  $m$  is the amount of the adsorbent in the desorption experiment (g); and  $q_e$  is the amount of Pb (II) adsorbed onto the adsorbent in the adsorption (mg/g) [Lu et al., 2019]. Desorption rates versus pH graphs were given in Figure 10.

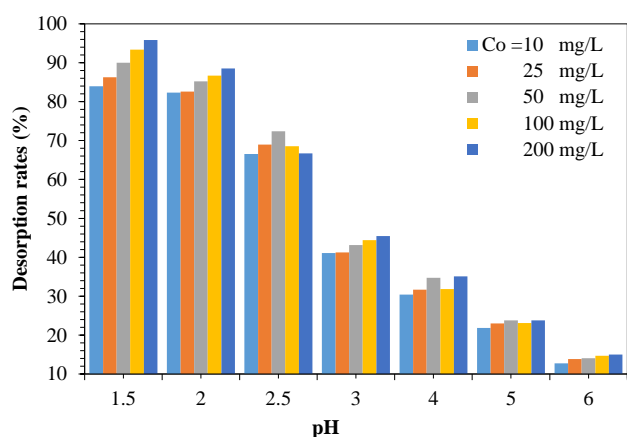


**Figure 10.** Desorption rates of RTB versus pH graph for 3 g/L adsorbent dosage.

As can be clearly seen from Figure 8, the desorption of lead from RTB is highly related to the pH of the solution. In this study, the maximum desorption rate was 95.85% at pH 1.5 for 3 g/L sorbent concentration. The desorption rates decreased rapidly (14.99% at pH 6) with increasing pH. In addition, desorption efficiencies increased with increasing adsorbent concentrations and initial Pb (II) concentrations. According to these results, it can be said that RTB is a reusable sorbent for removal of Pb (II).

## Conclusion

The RTB exhibited a good adsorption performance for Pb (II) with  $q_{max}$  of 188.16 mg/g. Maximum adsorption occurred at 30 °C for 3 g/L adsorbent and 10 mg/L initial Pb (II) concentration. It was observed that the adsorption process was pH dependent and the optimum pH for Pb (II) removal was 5.5. Since the Langmuir isotherm model correlates better than the

Freundlich model for the adsorption of Pb (II) on the RTB, the adsorption can be described as monolayer and reversible. According to pseudo-second-order kinetic data, the predominant adsorption process of Pb (II) was attributed to chemical reactions. Since Pb (II) can be desorbed with an efficiency of over 95%, RTB has been found to be a stable and reusable adsorbent. Although the relatively low surface area of the adsorbent used did not affect the adsorption efficiency much in this study, attempts to increase this area may result in higher heavy metal adsorption efficiencies.

Further studies in combination with different heavy metal species will be beneficial in terms of the widespread use of RTB in heavy metal adsorption.

## Acknowledgment

This research was carried out in Atatürk University Engineering Faculty Environmental Engineering Department research laboratories. The authors would like to thank the staff of Atatürk University East Anatolia High Technology Application and Research Centre (DAYTAM).

## Conflict of Interest

The author declares that there is no conflict of interest regarding the publication of this paper.

## References

- Abdelhafez, A. A., & Li, J. (2016). Removal of Pb(II) from aqueous solution by using biochars derived from sugar cane bagasse and orange peel. *Journal of the Taiwan Institute of Chemical Engineers*, 61, 367-375. <https://doi.org/10.1016/j.jtice.2016.01.005>
- Abdullah, N., Yusof, N., Lau, W. J., Jaafar, J., & Ismail, A. F. (2019). Recent trends of heavy metal removal from water/wastewater by membrane technologies. *Journal of Industrial and Engineering Chemistry*, 76, 17-38. <https://doi.org/10.1016/j.jiec.2019.03.029>
- Al-Ghamdi, Y. O., Alamry, K. A., Hussein, M. A., Marwani, H. M., & Asiri, A. M. (2019). Sulfone-modified chitosan as selective adsorbent for the extraction of toxic Hg(II) metal ions. *Adsorption Science and Technology*, 37(1-2), 139-159. <https://doi.org/10.1177/0263617418818957>
- Asadi, R., Abdollahi, H., Gharabaghi, M., & Boroumand, Z. (2020). Effective removal of Zn (II) ions from aqueous solution by the magnetic MnFe<sub>2</sub>O<sub>4</sub> and CoFe<sub>2</sub>O<sub>4</sub> spinel ferrite nanoparticles with focuses on synthesis, characterization, adsorption, and desorption. *Advanced Powder Technology*, 31(4), 1480-1489. <https://doi.org/10.1016/j.apt.2020.01.028>
- Awual, M. R., & Hasan, M. M. (2019). A ligand based innovative composite material for selective lead(II) capturing from wastewater. *Journal of Molecular Liquids*, 294, 111679. <https://doi.org/10.1016/j.molliq.2019.111679>

019.111679

- Bansal, M., Garg, U., Singh, D., & Garg, V. K. (2009). Removal of Cr(VI) from aqueous solutions using pre-consumer processing agricultural waste: A case study of rice husk. *Journal of Hazardous Materials*, 162(1), 312-320. <https://doi.org/10.1016/j.jhazmat.2008.05.037>
- Bardestani, R., Roy, C., & Kaliaguine, S. (2019). The effect of biochar mild air oxidation on the optimization of lead(II) adsorption from wastewater. *Journal of Environmental Management*, 240, 404-420. <https://doi.org/10.1016/j.jenvman.2019.03.110>
- Basu, M., Guha, A. K., & Ray, L. (2017). Adsorption of lead on cucumber peel. *Journal of Cleaner Production*, 151, 603-615. <https://doi.org/10.1016/j.jclepro.2017.03.028>
- Charoenchai, M., & Tangbunsuk, S. (2022). Effect of ternary polymer composites of macroporous adsorbents on adsorption properties for heavy metal removal from aqueous solution. *Environmental Science and Pollution Research*, 29, 84006-84018. <https://doi.org/10.1007/s11356-022-21701-0>
- Chen, X., Zhang, G., Li, J., & Ji, P. (2021). Possibility of removing Pb and Cd from polluted water by modified fly ash. *Adsorption Science and Technology*, 2021, 1336638. <https://doi.org/10.1155/2021/1336638>
- Chu, Y., Khan, M. A., Wang, F., Xia, M., Lei, W., & Zhu, S. (2019). Kinetics and equilibrium isotherms of adsorption of Pb(II) and Cu(II) onto raw and arginine-modified montmorillonite. *Advanced Powder Technology*, 30(5), 1067-1078. <https://doi.org/10.1016/j.apt.2019.03.002>
- Cid, H., Ortiz, C., Pizarro, J., & Moreno-Piraján, J. C. (2020). Effect of copper (II) biosorption over light metal cation desorption in the surface of macrocystis pyrifera biomass. *Journal of Environmental Chemical Engineering*, 8(3), 103729. <https://doi.org/10.1016/j.jece.2020.103729>
- Dąbrowski, A., Hubicki, Z., Podkościelny, P., & Robens, E. (2004). Selective removal of the heavy metal ions from waters and industrial wastewaters by ion-exchange method. *Chemosphere*, 56(2), 91-106. <https://doi.org/10.1016/j.chemosphere.2004.03.006>
- Demirbas, A. (2008). Heavy metal adsorption onto agro-based waste materials: A review. *Journal of Hazardous Materials*, 157(2-3), 220-229. <https://doi.org/10.1016/j.jhazmat.2008.01.024>
- Dubey, S. P., & Gopal, K. (2007). Adsorption of chromium(VI) on low cost adsorbents derived from agricultural waste material: A comparative study. *Journal of Hazardous Materials*, 145(3), 465-470. <https://doi.org/10.1016/j.jhazmat.2006.11.041>
- Edelstein, M., & Ben-Hur, M. (2018). Heavy metals and metalloids: Sources, risks and strategies to reduce their accumulation in horticultural crops. *Scientia Horticulturae*, 234, 431-444. <https://doi.org/10.1016/j.scienta.2017.12.039>
- FAO. (2022). *The state of world fisheries and aquaculture 2022: Towards blue transformation*. <https://doi.org/10.4060/cc0461en>
- Guan, J., Hu, C., Zhou, J., Huang, Q., & Liu, J. (2022). Adsorption of heavy metals by *Lycium barbarum* branch-based adsorbents: Raw, fungal modification, and biochar. *Water Science and Technology*, 85(7), 2145-2160. <https://doi.org/10.2166/wst.2022.067>
- Hayati, B., Maleki, A., Najafi, F., Daraei, H., Gharibi, F., & McKay, G. (2017). Super high removal capacities of heavy metals (Pb<sup>2+</sup> and Cu<sup>2+</sup>) using CNT dendrimer. *Journal of Hazardous Materials*, 336, 146-157. <https://doi.org/10.1016/j.jhazmat.2017.02.059>
- Ibrehem, A. S. (2019). Experimental and theoretical study to optimize rate constants of adsorption and desorption of the wastewater treatment using waste of tea plant. *Arabian Journal for Science and Engineering*, 44(8), 7361-7370. <https://doi.org/10.1007/s13369-019-03896-6>
- Kennedy, L. J., Vijaya, J. J., Sekaran, G., & Kayalvizhi, K. (2007). Equilibrium, kinetic and thermodynamic studies on the adsorption of m-cresol onto micro- and mesoporous carbon. *Journal of Hazardous Materials*, 149(1), 134-143. <https://doi.org/10.1016/j.jhazmat.2007.03.061>
- Khan, M. N., Ullah, H., Naeem, S., Uddin, J., Hamid, Y., Ahmad, W., & Ding, J. (2021). Remediation of emerging heavy metals from water using natural adsorbent: Adsorption performance and mechanistic insights. *Sustainability (Switzerland)*, 13(16), 8817. <https://doi.org/10.3390/su13168817>
- Kumar, M., Nandi, M., & Pakshirajan, K. (2021). Recent advances in heavy metal recovery from wastewater by biogenic sulfide precipitation. *Journal of Environmental Management*, 278, 111555. <https://doi.org/10.1016/j.jenvman.2020.111555>
- Liu, L., Li, W., Song, W., & Guo, M. (2018). Remediation techniques for heavy metal-contaminated soils: Principles and applicability. *Science of the Total Environment*, 633, 206-219. <https://doi.org/10.1016/j.scitotenv.2018.03.161>
- Liu, R., Guan, Y., Chen, L., & Lian, B. (2018). Adsorption and desorption characteristics of Cd<sup>2+</sup> and Pb<sup>2+</sup> by micro and nano-sized biogenic CaCO<sub>3</sub>. *Frontiers in Microbiology*, 9, 41. <https://doi.org/10.3389/fmicb.2018.00041>
- Lu, M., Zhang, Y., Zhou, Y., Su, Z., Liu, B., Li, G., & Jiang, T. (2019). Adsorption-desorption characteristics and mechanisms of Pb(II) on natural vanadium, titanium-bearing magnetite-humic acid magnetic adsorbent. *Powder Technology*, 344, 947-958. <https://doi.org/10.1016/j.powtec.2018.12.081>
- Martínez-Huitle, C. A., & Panizza, M. (2018). Electrochemical oxidation of organic pollutants for wastewater treatment. *Current Opinion in Electrochemistry*, 11(1), 62-71. <https://doi.org/10.1016/j.coelec.2018.07.010>

- Nadeem, M., Mahmood, A., Shahid, S. A., Shah, S. S., Khalid, A. M., & McKay, G. (2006). Sorption of lead from aqueous solution by chemically modified carbon adsorbents. *Journal of Hazardous Materials*, 138(3), 604-613. <https://doi.org/10.1016/j.jhazmat.2006.05.098>
- Qiao, Y., He, C., Zhang, C., Jiang, C., Yi, K., & Li, F. (2019). Comparison of adsorption of biochar from agricultural wastes on methylene blue and Pb<sup>2+</sup>. *BioResources*, 14(4), 9766-9780. <https://doi.org/10.15376/biores.14.4.9766-9780>
- Rice, E. W., Baird, R. B., Eaton, A. D., & Clesceri, L. S. (2012). *Standard methods for the examination of water and wastewater* (22<sup>nd</sup> ed.). American Public Health Association.
- Senthil Kumar, P., & Gayathri, R. (2009). Adsorption of Pb<sup>2+</sup> ions from aqueous solutions onto bael tree leaf powder: Isotherms, kinetics and thermodynamics study. *Journal of Engineering Science and Technology*, 4(4), 381-399.
- Silva-Yumi, J., Escudey, M., Gacitua, M., & Pizarro, C. (2018). Kinetics, adsorption and desorption of Cd(II) and Cu(II) on natural allophane: Effect of iron oxide coating. *Geoderma*, 319, 70-79. <https://doi.org/10.1016/j.geoderma.2017.12.038>
- Taha, A. A., Shreadah, M. A., Ahmed, A. M., & Heiba, H. F. (2016). Multi-component adsorption of Pb(II), Cd(II), and Ni(II) onto Egyptian Na-activated bentonite; Equilibrium, kinetics, thermodynamics, and application for seawater desalination. *Journal of Environmental Chemical Engineering*, 4(1), 1166-1180. <https://doi.org/10.1016/j.jece.2016.01.025>
- Tongtavee, N., Loisuangsri, A., & McLaren, R. G. (2021). Lead desorption and its potential bioavailability in soil used for disposing lead-contaminated pomelo peel: Effects of contact time and soil pH. *Water, Air, and Soil Pollution*, 232, 384. <https://doi.org/10.1007/s11270-021-05344-4>
- Toppe, J., Albrektsen, S., Hope, B., & Aksnes, A. (2007). Chemical composition, mineral content and amino acid and lipid profiles in bones from various fish species. *Comparative Biochemistry and Physiology - B Biochemistry and Molecular Biology*, 146(3), 395-401. <https://doi.org/10.1016/j.cbpb.2006.11.020>
- TÜİK. (2022). *Su ürünleri*. <https://data.tuik.gov.tr/Bulten/Index?p=Su-Urunleri-2021-45745> (In Turkish)
- Wang, Q., Wang, B., Lee, X., Lehmann, J., & Gao, B. (2018). Sorption and desorption of Pb(II) to biochar as affected by oxidation and pH. *Science of the Total Environment*, 634, 188-194. <https://doi.org/10.1016/j.scitotenv.2018.03.189>
- Wang, Y., Wang, X., Wang, X., Liu, M., Wu, Z., Yang, L., Xia, S., & Zhao, J. (2013). Adsorption of Pb(II) from aqueous solution to Ni-doped bamboo charcoal. *Journal of Industrial and Engineering Chemistry*, 19(1), 353-359. <https://doi.org/10.1016/j.jiec.2012.08.024>
- Xie, S., Wen, Z., Zhan, H., & Jin, M. (2018). An experimental study on the adsorption and desorption of Cu(II) in silty clay. *Geofluids*, 2018, 3610921. <https://doi.org/10.1155/2018/3610921>
- Yu, M., Zhu, B., Yu, J., Wang, X., Zhang, C., & Qin, Y. (2022). A biomass carbon prepared from agricultural discarded walnut green peel: Investigations into its adsorption characteristics of heavy metal ions in wastewater treatment. *Biomass Conversion and Biorefinery*. <https://doi.org/10.1007/s13399-021-02217-y>
- Yun, Y. S., Park, D., Park, J. M., & Volesky, B. (2001). Biosorption of trivalent chromium on the brown seaweed biomass. *Environmental Science and Technology*, 35(21), 4353-4358. <https://doi.org/10.1021/es010866k>
- Zhang, J., Shao, J., Jin, Q., Li, Z., Zhang, X., Chen, Y., Zhang, S., & Chen, H. (2019). Sludge-based biochar activation to enhance Pb(II) adsorption. *Fuel*, 252, 101-108. <https://doi.org/10.1016/j.fuel.2019.04.096>
- Zhu, S., Xia, M., Chu, Y., Khan, M. A., Lei, W., Wang, F., Muhmood, T., & Wang, A. (2019). Adsorption and desorption of Pb(II) on L-Lysine modified montmorillonite and the simulation of interlayer structure. *Applied Clay Science*, 169, 40-47. <https://doi.org/10.1016/j.clay.2018.12.017>